Frontiers + Innovation
2009 CSPG CSEG CWLS CONVENTION • CALGARY, ALBERTA, CANADA

Near-surface Issues in TTI Wave Equation Migration from Topography

Chuck Ursenbach*, Richard A. Bale, and Samuel H. Gray
CGGVeritas, Calgary, Canada
Charles.Ursenbach@cggveritas.com

Summary

Wave-equation migration, which uses more accurate wavefield extrapolation techniques than ray-based Kirchhoff migration, produces high-quality images beneath complex overburdens. However, near-surface images resulting from wave equation methods are sometimes less satisfactory than those from Kirchhoff migration, even though more computing effort is required to obtain them. Two filters are shown to be useful in improving the near surface image: a *k*-filter with an elliptical cutoff, and a subsurface *p*-filter. In addition, it is useful to introduce a zero-slowness layer in connection with topography.

Introduction

The current standard for migration of Alberta Foothills data is the 3D Kirchhoff method adapted to tilted transverse isotropy (TTI). The 3D coverage is necessary to image intricate subsurface structure, while TTI is necessary to obtain accurate kinematics. This generally yields a faithful description of the near surface, but there is interest in wavefield extrapolation methods that could be more reliable for structures buried below a complex overburden.

Wave equation migration (WEM) holds promise for such a purpose, and has shown the ability to produce superior images at depth (Bale and Gray, 2008). However the near-surface results have often been less satisfactory than those of Kirchhoff, despite the greater computing resources required.

We demonstrate that improvement of the near surface can be obtained through various filtering approaches, and that the concept of a 'zero-slowness' layer can be useful in migrating from topography.

Theory

The methods of TTI wave equation migration have been presented earlier (Bale et al. 2007a,b; Bale and Gray, 2008). Here we present only a discussion of filtering and topography.

K-filtering

2D spatial FFTs are an important component of 3D phase-shift WEM. However, spurious noise can be introduced along the *x* and *y* axis directions in various ways, such as when the inverse transform leads to a narrow, high-amplitude spike in real space, as shown in Figure 1. Using a rectangular *k*-filter may mask this to some extent, but a better result is achieved if the filter has an elliptical cutoff. Similar coherent noise can be present in migrated images. It may appear for different reasons than here, but can be treated similarly.

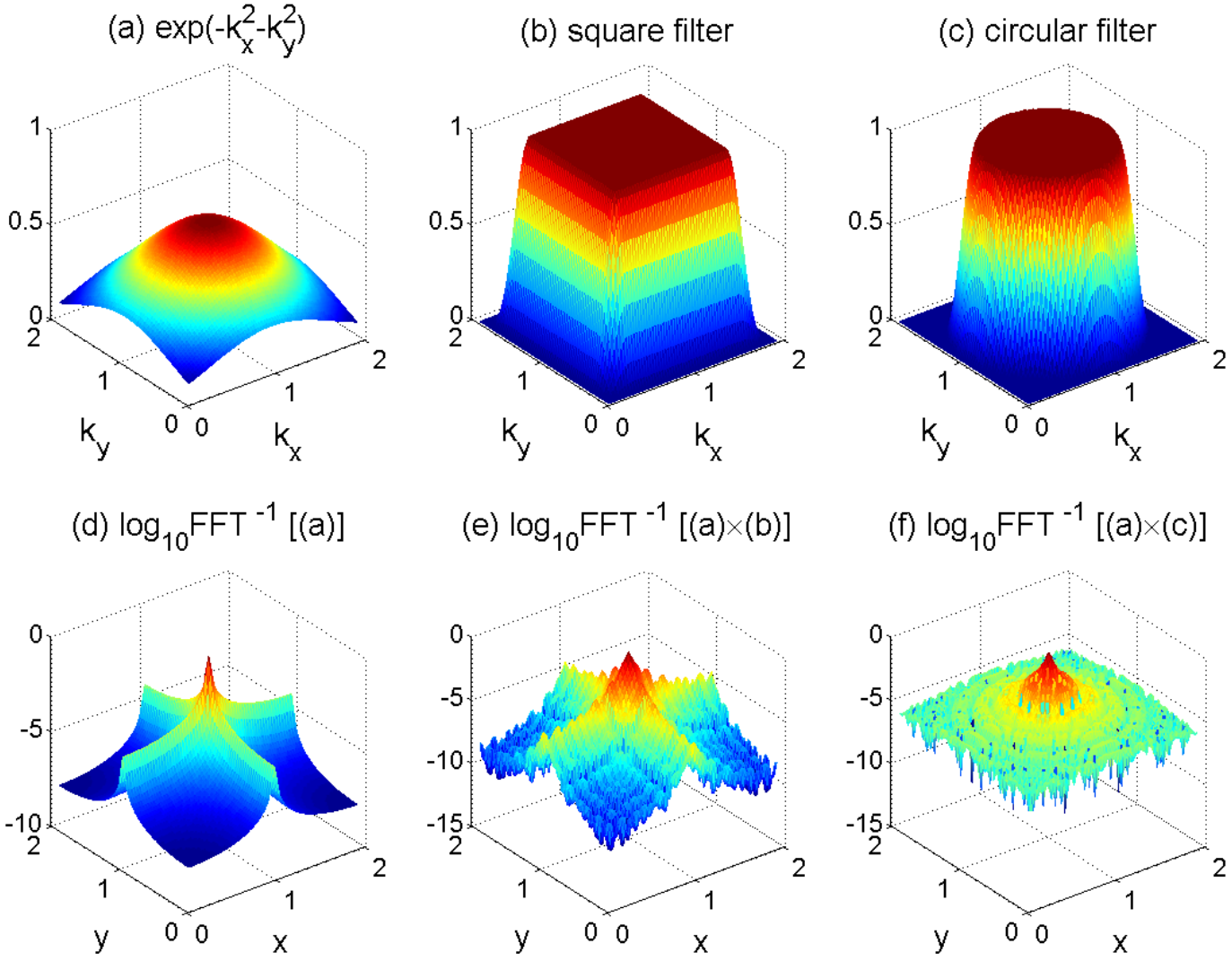

Figure 1: (a) A Gaussian function in *k*-space, which still has noticeable amplitude at grid edges. (b) A product of cosine-tapered filters in *x* and *y* directions. (c) A radial cosine-tapered filter. (d) The inverse transform of truncated Gaussian. (e) The inverse transform of square-filtered Gaussian. (f) The inverse transform of radially-filtered Gaussian. Parts (d)-(f) show the base-10 log of the absolute value of the real-space function, as a small imaginary component results from the finite size of the domain.

Subsurface angle and slowness filtering

This filtering is based on the relation $\sin\theta = \frac{k_h v}{\omega}$, where $\theta, k_h, v,$ and ω represent angle with respect to vertical, horizontal wavenumber, wavespeed, and frequency. A migration operator generates image components at all angles and, with adequate sampling, these combine to yield image components descriptive of the subsurface. When sampling is not ideal, it may be advantageous to remove some of the higher angle components which could persist as artefacts in the final image. This is accomplished in Fourier space by setting a cutoff value of θ (angle filtering) or $\sin\theta/v$ (horizontal slowness filtering) and then removing wavenumber components of the data prohibited by this cutoff.

Zero-slowness layer

WEM methodology is readily applied when the surface can be treated as perfectly flat. In Foothills surveys the topography is often too pronounced for this assumption, and it is not obvious how to proceed. Consequently a variety of solutions have been proposed. The first method that was both accurate and efficient was applied to finite-difference methods and employed a zero-velocity layer (Beasley and Lynn, 1989, 1992; Gray, 1997). Reshef (1991) presented a different method for use with phase-shift algorithms.

In his method a *non-zero* velocity is employed above topography, a zeroed receiver wavefield is initiated at the flat datum, and then observed data are added into this wavefield as it propagates past various receiver stations. A similar approach is to move all observed data to the flat datum and propagate downward, but at each step to replace the propagated wavefield with its original value for that (x,y) location, until it descends below the surface at that location.

All of these methods are valid as described. However, in these methods it is often assumed that every grid cell is entirely above or below topography. Ng (2007,2008) has observed that this assumption severely limits depth step size. He proposes a novel solution in which a post-propagation static correction is used to approximately account for the fact that propagation occurs through only a portion of the cell. Alternatively we show that one can treat the straddling cells in the propagation step as well. This can be done by assigning an *infinite* wavespeed above the surface. If the depth step Δz is the sum of Δz_1 and Δz_2, representing the thicknesses of the regions above and below the surface, then the average slowness of the cell is $(\Delta z_2 / \Delta z)(1/v)$. Because no change is desired in the wavefield in the Δz_1 interval (above topography), the ideal (isotropic) propagator for this depth step would be $\exp\left[i\Delta z_2\sqrt{(\omega/v)^2 - k_h^2}\right]$. By comparison, the propagator for the full depth step, using the average slowness, can be expressed as $\exp\left[i\Delta z_2\sqrt{(\omega/v)^2 - (k_h \Delta z/\Delta z_2)^2}\right]$. The two expressions are identical for the $k_h = 0$ component of the wavefield, so the correct static shift is obtained, while the errors in non-zero k_h components typically have negligible effect over lateral distances greater than the trace spacing. This permits the use of larger depth steps.

Examples

Here we present some examples of the above methods using the Copton Foothills 3D seismic survey (Bale and Gray, 2008).

K-filtering

Noise along the x and y axes can be quite apparent in 3D single migrated impulses. In stacked images it is masked at depth, but is still visible at the surface (perhaps more so at irregular surfaces). Figure 2 shows the effect on this noise of applying either a rectangular or elliptical k-filter. The filters are applied at every depth on both source and receiver wavefields, and differences are obvious at the surface, but less noticeable further down.

(a) 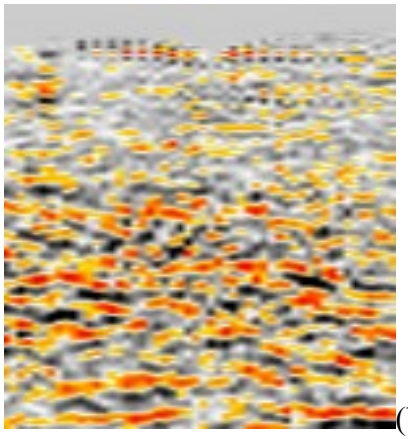 (b) 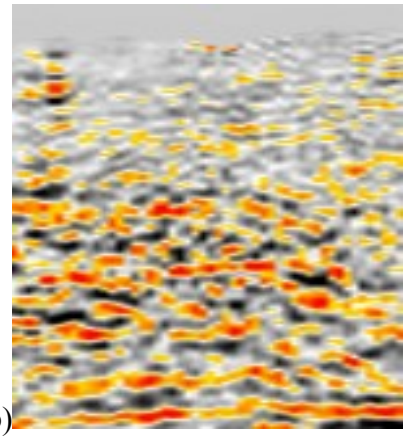 (c) 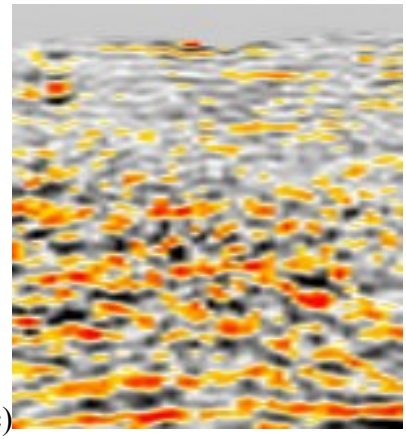

Figure 2: (a) Unfiltered image (40 Hz), extracted from Copton TTI WEM migration. (b) Same as (a), but with rectangular filter applied. (c) Same as (a), but with elliptical filter applied

Subsurface slowness filtering

Events in the image near the surface are vulnerable to corruption by high-angle arms of the migration operator, as seen in Figure 3a. Applying a p-filter (Figure 3b) mutes these artefacts to show flat events more clearly. Caution must be used though as high-angle events will also be weakened.

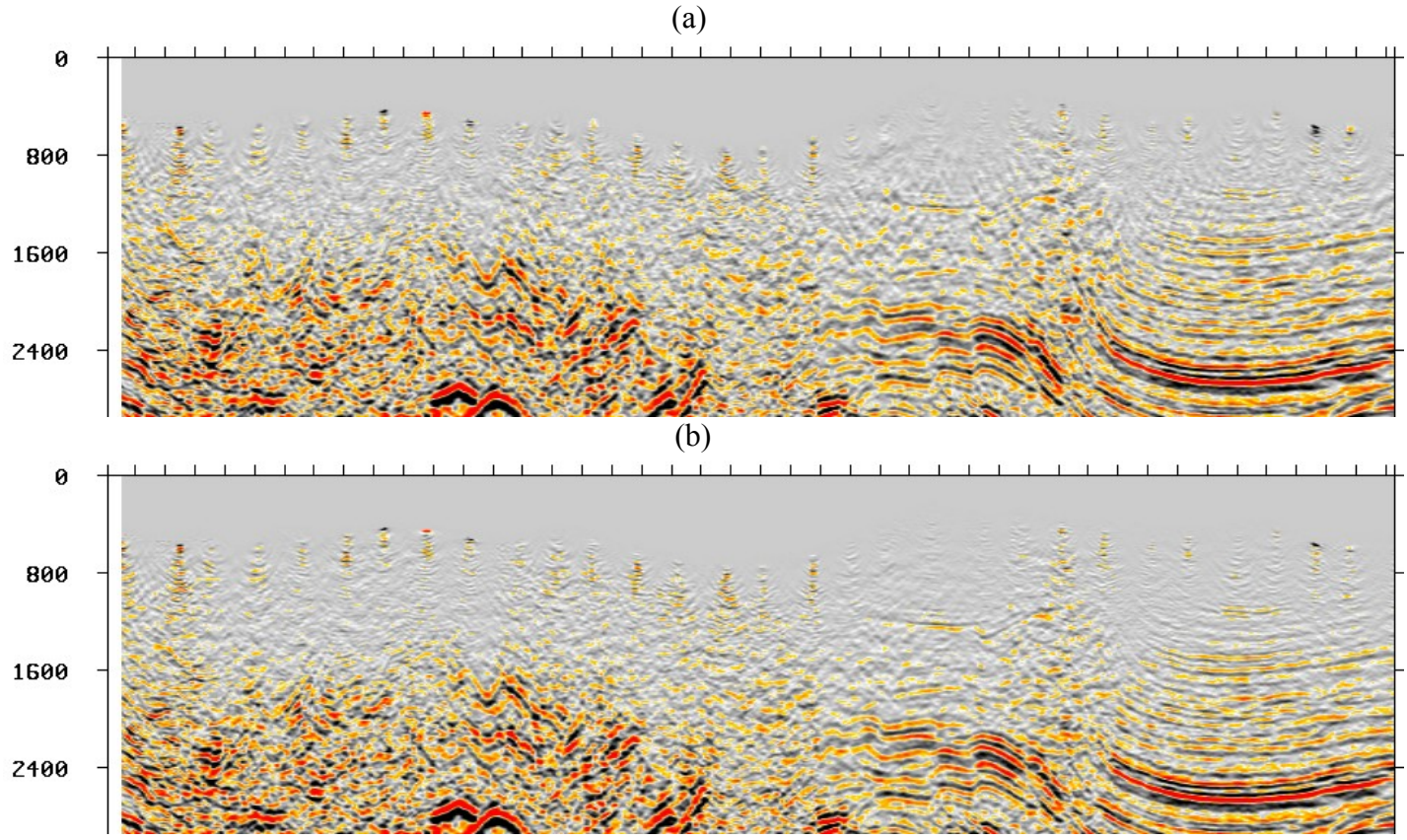

Figure 3: (a) Near-surface portion of Copton migration image (70 Hz, 1000 m AGC) with only *k*-filtering applied (elliptical cutoff). (b) Same as (a) but also with *p*-filter cutoff of 0.000205 s/m.

Zero-slowness layer

The above calculations were carried out using a TTI adaptation of the zero-slowness layer described above.

Conclusions

Careful use of filtering can improve the quality of near-surface images for TTI WEM. The zero-slowness concept permits the use of large depth steps even in datasets with extensive topography.

References

Bale, R. A., Gray, S. H., and Kirtland-Grech, M. G., 2007a, TTI Wave Equation Migration by Phase-Shift Plus Interpolation: National Convention, Canadian Society of Exploration Geophysicists, Expanded Abstracts, 414-417.

Bale, R. A., Gray, S. H., and Kirtland-Grech, M. G., 2007b, TTI Wave Equation Migration: 77th Annual International Meeting, Society of Exploration Geophysicists, Expanded Abstracts, 2295-2299.

Bale, R. A., and Gray, S. H., 2008, TTI Wave Equation Migration of a 3-D Canadian Foothills Dataset: National Convention, Canadian Society of Exploration Geophysicists, Expanded Abstracts, 339-343.

Beasley, C., and Lynn, W., 1989, Zero-velocity layer: Migration from irregular surfaces: 59th Annual International Meeting, Society of Exploration Geophysicists, Expanded Abstracts, 1179-1183.

Beasley, C., and Lynn, W., 1992, The zero-velocity layer: Migration from irregular surfaces: Geophysics, **57**, 1435-1443.

Gray, S. H., 1997, Where is the zero-velocity layer?: Geophysics, **62**, 266-269.

Ng, M., 2007, A simple way to speed up wave equation migration: using a time-shift imaging condition: CSEG Recorder, **32**, 44-48.

Ng, M., 2008, A fast and accurate migration from topography via coarse step downward wavefield extrapoloation: 78th Annual International Meeting, Society of Exploration Geophysicists, Expanded Abstracts, SPMI P2.4.

Reshef, M., 1991, Depth migration from irregular surfaces with depth extrapolation methods: Geophysics, **56**, 119-122.